J Appl Electrochem (2010) 40:1365–1370
DOI 10.1007/s10800-010-0103-0

ORIGINAL PAPER

High temperature lithium cells using conversion oxide electrodes

**Francesc Mestre-Aizpurua · Stéphane Laruelle ·
Sylvie Grugeon · Jean-Marie Tarascon ·
M. Rosa Palacín**

Received: 23 September 2009 / Accepted: 14 February 2010 / Published online: 1 March 2010

Abstract Oxidized stainless steel electrodes containing chromium oxides without any conducting additives or binder have been successfully cycled at high temperatures (up to 100 °C) in organic solvent-based electrolytes with high reversibility. Cycling at high temperature results in an enhancement of the capacity at lower voltages, which is maintained upon cycling. After studying different electrolyte candidates, the best results were obtained using lithium bis(trifluoromethanesulfonyl)imide (LiTFSI) dissolved in ethylene carbonate.

Keywords Lithium batteries · High temperature electrochemistry · Iron chromium oxide · TFSI · Stainless steel · Conversion electrodes

1 Introduction

Tough lithium ion batteries have conquered the realm of portable electronics; their performance still falls short of the requirements to enter both transportation and stationary applications (including storage of renewable energy). Indeed, a need exists to develop advanced battery technologies with characteristics such as high energy and power densities, long life, low cost, and a high degree of safety. There is general agreement that breakthroughs in this field will not come from incremental improvements in existing technologies but from the development of novel chemistries and concepts.

Electrode materials based in conversion reactions are mainly binary compounds of general formula M_aX_b ($X = O, F, P, N, H,\ldots$) that react with lithium according to:

$$M_aX_b + (b \times n)Li \Leftrightarrow aM^\circ + bLi_nX$$

where n is the formal oxidation state of X^{n-} anions.

Such type of reactions enable full utilization of all the redox potentials of the host metals that are reduced to metal nanoparticles embedded in a matrix of the corresponding Li–X binary phase (Li_2O, LiF, Li_3P, Li_3N, LiH,…) [1–8]. This reduction to the metallic state brings about multiple alkaline ion/electron transfer in comparison to current insertion compounds that are mostly limited to one alkaline ion/electron per 3d-metal. Thus, a huge increase in specific capacity of lithium batteries would be achieved if implementation of these materials were possible. However, this is hampered by the large voltage hysteresis displayed by these systems. Poor ionic conductivity of the composite electrode may play a role to that respect, since electronic conductivity is relatively high along the full potential range of electrode operation [9]. If this was the case, we should expect significant reduction of the hysteresis with an increase of the operating temperature. Our aim being to test conversion reaction electrodes at high temperatures, the first step was to define the optimum electrode material and the best electrolyte to carry out such tests. This was done by taking into account thermal stabilities of the different solvents and salts [10]. Ethylene carbonate (EC) was chosen as solvent in view of its high boiling point and thermal stability combined with its low degradation at high temperature. Indeed, EC/salt electrolytes recovered from post mortem stainless steel/lithium cells cycled up to 75 °C have shown, at worst, traces of oligomeric PEG species,

F. Mestre-Aizpurua · M. R. Palacín (✉)
Institut de Ciència de Materials de Barcelona (ICMAB-CSIC),
Campus UAB, 08193 Bellaterra, Catalonia, Spain
e-mail: rosa.palacin@icmab.es

S. Laruelle · S. Grugeon · J.-M. Tarascon
Laboratoire de Réactivité et de Chimie des Solides, UMR CNRS
6007, 33 rue Saint Leu, 80039 Amiens Cedex 9, France

coming from solvent degradation [11]. Besides, better high temperature resilience of cells has been experienced using electrolyte formulations with high EC content [12]. Regarding salts, lithium tetrafluoroborate or lithium bis(trifluoromethanesulfonyl)imide, the latter currently abbreviated as LiTFSI, were chosen after cyclic voltammetry studies in EC at different temperatures. With respect to the electrode material, thick film metal oxide electrodes prepared through oxidation of stainless steel [13, 14] were selected for the sake of simplicity, since these electrodes do not contain any binder or conductive additives that could promote side reactions with the electrolytes at high temperatures and thus interfere with the interpretation of the results. The electrochemical reaction mechanism versus lithium for the oxidized stainless steel electrodes using 1 M $LiPF_6$ in EC:DMC as electrolyte has been discussed in detail in [14] both at room temperature and 55 °C. In agreement with other conversion reaction materials, the first reduction entails the formation of metal nanoparticles embedded in a Li_2O matrix, while first reoxidation is not fully reversible and does not allow the reconstruction of the pristine oxidized phase but rather leads to nano-sized oxide particles in which the transition metal is nearly in a +2 formal oxidation state. For these complex electrodes, the reduction reaction involves the formation of chromium nanoparticles and bimetallic alloy nanoparticles, from the two phases initially present at the electrode.

$$Cr_2O_{3\,\mathrm{bulk}} + 6Li \Rightarrow 2Cr^{\circ}_{\mathrm{nano}} + 3Li_2O$$

$$(Fe_xCr_{1-x})Cr_2O_4 + 8Li \Rightarrow 3\left(Fe_{x/3}Cr_{1-x/3}\right)^{\circ}_{\mathrm{nano}} + 4Li_2O$$

While upon further oxidation, a mixture of CrO and $Fe_yCr_{1-y}O$ ($y = x/3$) is formed.

$$Cr^{\circ}_{\mathrm{nano}} + Li_2O \Leftrightarrow CrO_{\mathrm{nano}} + 2Li$$

$$\left(Fe_yCr_{1-y}\right)^{\circ}_{\mathrm{nano}} + Li_2O \Leftrightarrow Fe_yCr_{1-y}O_{\mathrm{nano}} + 2Li$$

These electrochemical reactions come with concomitant capacity loss of at least 25 and 33% for $Fe_xCr_{3-x}O_4$ and $(Fe_xCr_{1-x})_2O_3$ phases type, respectively (see Fig. 1). The partial re-oxidation of the metals to the +2 state leaves residual Li_2O into the composite surrounding the nanoparticles. This Li_2O phase could act as insulator enhancing the polarization as well as oxygen reservoir. Hence, we considered to increase the operation temperature that could bring about a decrease in voltage hysteresis and allow complete re-oxidation of the electrodes and thus increase the energy efficiency.

Indeed, in the voltage window from 0 to 3 V, it was not possible to reoxidize the electrode material further; hence, we considered to increase the operation temperature. That could bring about a decrease in voltage hysteresis that would be sufficient to allow complete reoxidation of the electrodes and thus increase the energy efficiency.

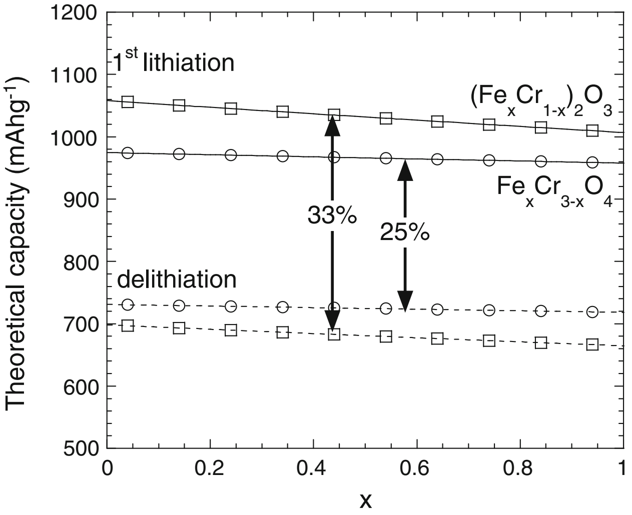

Fig. 1 Theoretical specific capacities of $(Fe_xCr_{1-x})_2O_3$ and $Fe_xCr_{3-x}O_4$ phases with $0 < x < 1$ for the first lithiation/delithiation cycle considering re-oxidation of the nano-sized metal particles limited to the +2 oxidation state

2 Experimental

Chromium-rich oxidized stainless steel electrodes were fabricated as reported elsewhere [13] by treating stainless steel wire mesh (mesh is 25 × 25 μm^2 and the diameter of wire was 25 μm) at 700 °C for 6 h under N_2/H_2 (90/10 v/v). SEM micrographs before and after heating treatment (Fig. 2) reveal the formation of a film with thickness close to 300 nm as deduced from previous GD-OES measurements [13]. HRTEM experiments [14, 15] revealed that the film is composed of Cr_2O_3 and a mixed oxide $(Fe_xCr_{1-x})Cr_2O_4$ ($0.3 < x < 1$). LiTFSI (Aldrich, ≥99.95%), $LiBF_4$ (Aldrich, 98%), and $LiClO_4$ (Aldrich, 95%) electrolyte salts were used as received. EC was purchased from Fluka (≥99.0%) and used to prepare 1 M electrolyte solutions of the corresponding salt inside an argon filled glove-box. Commercial 1 M $LiPF_6$ in EC:DMC 1:1 was purchased from Merck.

Electrochemical experiments at 150 °C were made using an in house specially designed high temperature electrochemical cell [16], whereas those carried out at lower temperatures could alternatively be carried out using standard Swagelok cells [17] with Teflon™ gaskets. The separator consisted of two sheets of Whattman GF/d borosilicate glass fiber soaked with the electrolyte while the negative electrode consisted of lithium metal foil (0.38 mm thick, Aldrich, 99.9%). Cyclic voltammetry experiments to determine the electrochemical stability limits of the electrolytes at working temperatures were performed at a 1.0 mV s^{-1} scan rate after a first fast cycle at 20 mV s^{-1}. In this case, the plunger current collector of the cell served as the working electrode (surface 1.1 cm^2).

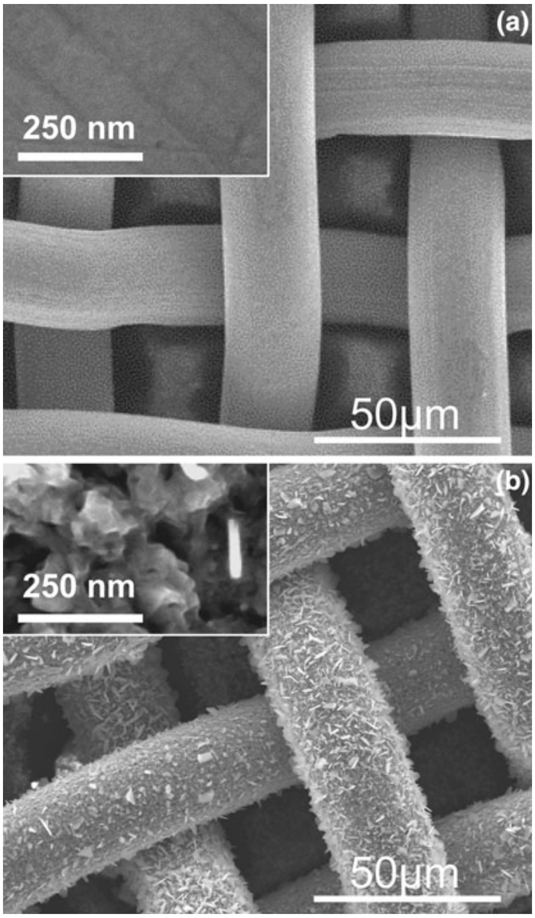

Fig. 2 SEM micrographs corresponding to the stainless steel wire mesh **a** before and **b** after treatment at 700 °C for 6 h under N_2/H_2 (90/10 v/v) flow

Cycling experiments were carried out at two different intensities, namely 1 and 0.2 mA cm^{-2}, and in this case 0.3 cm^2 disks cut from as prepared oxidized stainless steel were used as positive electrodes. All electrochemical experiments were made using either a Mac-Pile or a VMP3 potentiostat (Bio-Logic, France).

3 Results and discussion

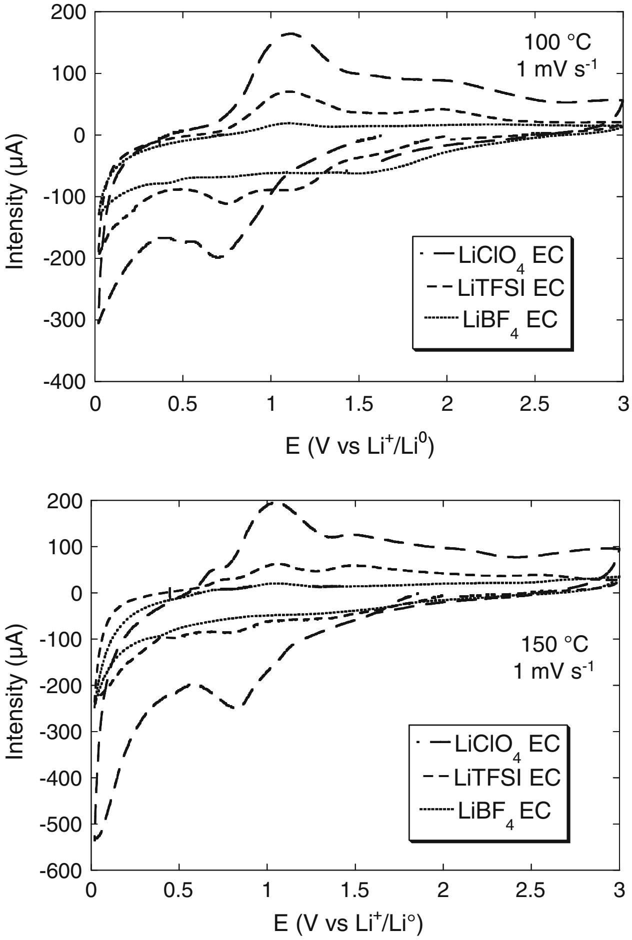

Fig. 3 Cyclic voltammetry experiments between OCV, 0 and 3 V carried out at 100 and 150 °C with a 1 mV/s scan rate corresponding to $LiBF_4$ in EC and LiTFSI in EC as electrolytes

In order ascertain the behavior of the electrolyte at high operation temperatures (100–150 °C), cyclic voltammetry experiments were conducted on the same Swagelok cells that were used for cycling experiments, with lithium metal at the counter and reference electrode, but without the electrochemically active stainless steel electrodes. The cyclic voltammetries between 0 and 3 V versus Li^+/Li^0 are shown in Fig. 3. As expected, the maximum decomposition current depends on the temperature, being higher at 150 °C. The lower thermal stability of $LiClO_4$ manifests itself with a much larger decomposition current, and the cathodic stability is, as expected much lower, in agreement with the tendency of $LiClO_4$ to get reduced and form $LiClO_x$ ($x < 4$), the final product being LiCl [18]. A large cathodic peak is observed around 0.8 V at 100 °C and around 0.7 V at 150 °C, while a large anodic peak is observed at around 1 V at 100 °C and 1.1 V at 150 °C. The two other salts do not differ markedly from each other (tough the decomposition current is slightly higher for LiTFSI than for $LiBF_4$). The fact that the voltammograms corresponding to LiTFSI exhibit more distinct anodic and cathodic peaks points to a participation of the TFSI anions in SEI formation, which is in agreement with previous studies carried out at room temperature [19]. Two cathodic peaks are observed at ca. 1.1 and 0.8 V at 100 °C and at ca. 1.2 and 0.80 V at 150 °C while two anodic peaks are observed at about 1.9 and 1.1 V at 100 °C and three anodic peaks at 0.7, 1.4, and 1.1 V at 150 °C. The investigation of the exact processes taking place is a complex task beyond the scope of this paper. However, cyclic voltammetry experiments allowed us to ascertain that the oxidation currents for LiTFSI and $LiBF_4$ are always under 50 µA cm^{-2} and the reduction current values under 250 µA cm^{-2} and hence both electrolytes can be considered to be stable in this voltage window.

In view of the above-mentioned results, high temperature cycling experiments were thus performed using both $LiBF_4$ in EC and LiTFSI in EC electrolytes at 100 and 150 °C. Unfortunately, we only succeeded in achieving prolonged cycling at 100 °C since all cells tested at 150 °C failed in the very first cycles. This might relate to an enhanced degradation of the electrolyte due to contact with the oxide electrodes that can catalyze decomposition, especially at such high temperatures. Indeed, electrochemical stability limits for electrolytes are usually evaluated using inert electrodes and they may not hold in the presence of other faradaic processes. Experiments at 100 °C were successful in all cases, tough cells using $LiBF_4$ as electrolyte failed after 20 cycles and sustained cycling could only be achieved with LiTFSI, certainly due to its enhanced thermal stability [20]. Figure 4 shows the plots of capacity versus cycle number for experiments carried out at 100 °C with both electrolytes, together with those carried out with the standard electrolyte ($LiPF_6$ in EC/DMC) at room temperature and with LiTFSI in EC at 50 °C for comparative purposes. In agreement with previous results [14], capacity values under 0.2 mA h cm^{-2} are obtained at room temperature with $LiPF_6$ in EC/DMC and also (though slightly higher) at 50 °C with LiTFSI in EC. A decrease in current density induces, as expected, an increase in capacity in all cases. The most remarkable feature is, however, the increase in the electrochemical capacity with increasing the operation temperature. First, the capacity on the first reduction is enhanced from about 0.3 mA h cm^{-2} at room temperature to about 0.4 mA h cm^{-2} at 100 °C. Assuming a density close to 5 g cm^{-3} for the oxide film (350 nm thick) grown on the stainless steel wire mesh having a cumulated surface of 3 cm^2 per geometrical square centimeter, a maximum capacity of mA h cm^{-2} could be roughly calculated. Hence, we suppose that all the conversion reaction capacity could be almost achieved at room temperature during the first reduction. The capacity upon subsequent oxidation is only slightly increased from 0.17 to 0.2 mA h cm^{-2}. This seems to indicate that the first delithiation process still leads to the formation of simple oxide (CrO or $Fe_yCr_{1-y}O$) with metals in a +2 oxidation state.

Upon cycling, capacity at 100 °C is found to progressively increase, doubling the values obtained at room temperature at 60 cycles (multiplying by 5 at 150 °C). Moreover, in the case of $LiBF_4$, slightly higher capacities are obtained upon reduction, but for LiTFSI no significant differences are observed between capacity values achieved on charge and on discharge except for the first reduction. Thus, even if there is a significant irreversible capacity during the first cycle, the coulombic efficiency is close to 100% afterward with reduction capacities being slightly

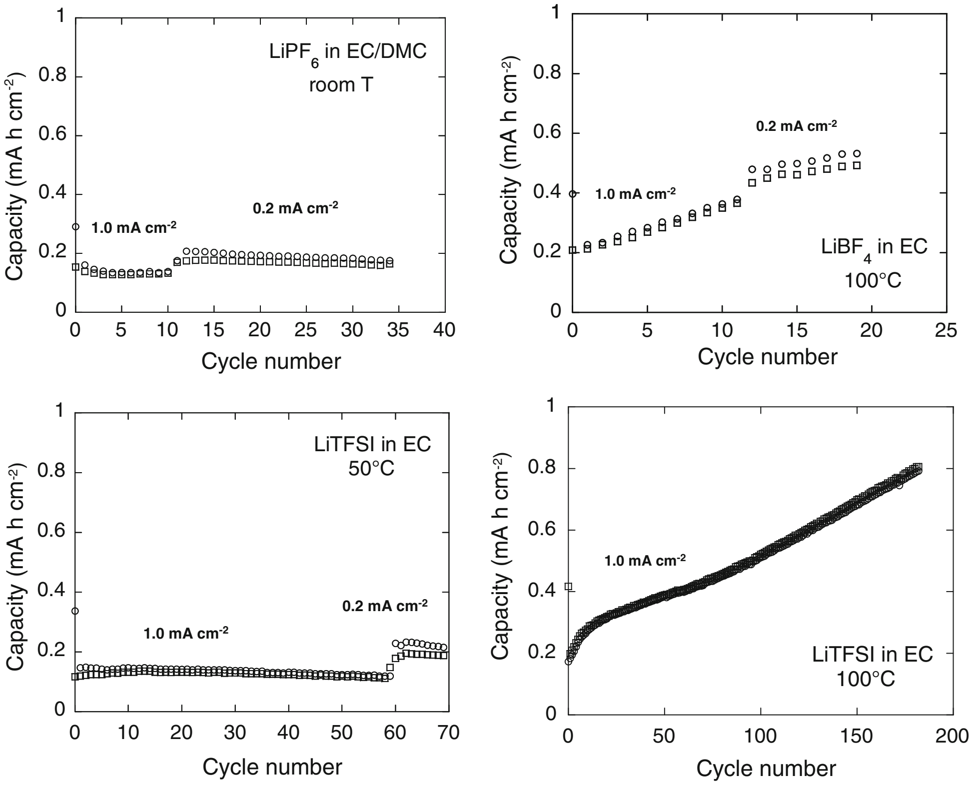

Fig. 4 Capacity versus cycle number plots for cells cycled at different temperatures with the electrolytes and current densities specified

higher, and electrodes can be successfully submitted to long cycling at this temperature (see Fig. 4) with capacity *increasing* upon cycling. This gain in capacity upon cycling could be due to an increased amount of active material due to enhanced corrosion of the electrode, but the fact that most TFSI salts are expected to be soluble in the electrolyte [21] makes this hypothesis questionable. Otherwise, and also in order to explain the gain in capacity, we could also bring into play an improved reversibility of the redox reaction upon cycling leading to recovery of oxides with the metals in higher oxidation states than +2 upon oxidation; finally, the so-called extra capacity at low voltages could gradually be extended at high *T*. This extra capacity may correspond to one or several reduction processes taking place at the electrode besides the conversion one. We could expect that a part of this capacity to be reversible. Two alternative explanations have been proposed for such phenomenon: (i) the first, based on TEM and analytical investigations, ascribes this extra capacity to the electrochemical reduction of electrolyte solvents leading to the chemical formation of a polymeric layer at the electrode [22] that is redissolved upon oxidation through an unclear reaction [23]; (ii) the second proposes the existence of a highly reversible novel pseudocapacitive mechanism termed lithium interfacial storage wherein charge would be stored at the interfaces of the extremely small Li_2O/metal nanograin domains (Li^+ ions in the surface of Li_2O and electrons in the surface of transition metal nanograins, respectively), akin to the so-called UPD (underpotential deposition) of Li [24, 25]. Figure 5 shows the voltage versus capacity plot corresponding to the first cycle of the experiments reported in Fig. 4. Interestingly, a large voltage hysteresis is still observed at 100 °C with both electrolytes, thus indicating that such increase in temperature is not sufficient to have a significant effect. From the examination of the plots, it can clearly be seen that the increase in capacity with temperature is achieved at very low voltages bearing out the increased extra capacity hypothesis. Lower reversible capacity is observed for electrodes using LiTFSI in EC at 50 °C when compared to $LiPF_6$ in EC/DMC, most probably due to the lower ionic conductivity of the former and possibly higher viscosity with poorer wetting of nanopores. However, by increasing the operation temperature to 100 °C, the irreversible capacity in this first cycle is roughly the same (close to 0.15 mA h cm^{-2}), which indicates that these ionic limitations do not exist anymore and also that the final oxidation state for the metals at the end of charge is the same. This can also be deduced from the corresponding derivative curves (not shown). The behavior of the cell at 100 °C is highly reversible after the initial capacity loss, which indicates that this extra capacity is highly reversible as well. Indeed, from the plot in Fig. 4, it can clearly be seen that capacities on oxidation and on reduction are almost the same. This balance is striking if the formation and dissolution of a polymeric layer are still to be invoked, since the processes of electrolyte reduction to form the polymeric layer and further oxidation of that layer, if any, are obviously not the same and hence probably not involving the same amount of charge. Hence, this supposes that the polymeric layer dissolution upon charge does not involve any electrochemical process as initially suggested and only electrolyte reduction could explain the slightly enhanced discharge capacity upon cycling (and more extra capacity upon the first discharge to form SEI). Even if the origin of such phenomenon is still an open question beyond the scope of this paper, it is clear that it is enhanced by temperature and highly reversible upon cycling.

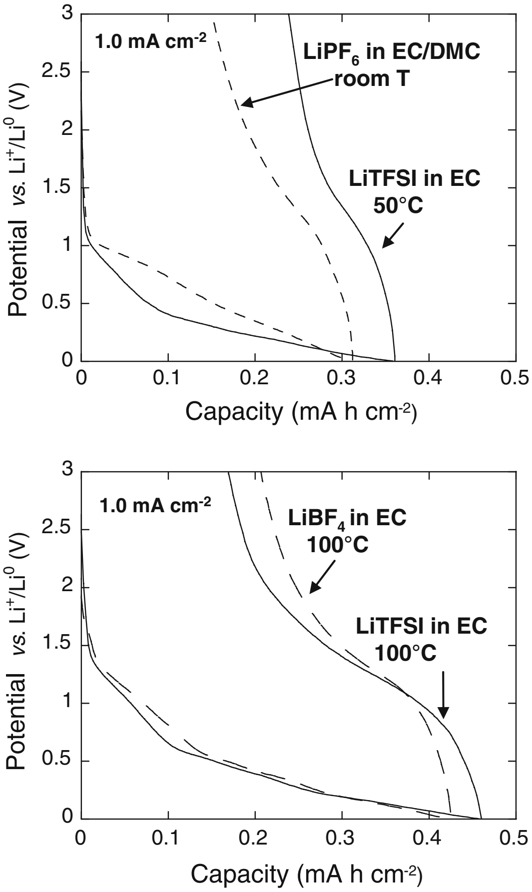

Fig. 5 Voltage versus composition plot for the first cycle of the experiments depicted in Fig. 4

4 Conclusions

In summary, our study proves that oxidized stainless steel electrodes are suitable for cycling at high temperatures (up to 100 °C) in organic solvent-based electrolytes with high reversibility. These results are not only of fundamental interest but also to be taken into account if rechargeable lithium batteries able to work at high temperature for some specific applications [26] such as electronics for oil drilling, are to be developed.

Acknowledgments The authors are indebted to the ALISTORE Network of Excellence (EC, SES6-CT-2003-503532) for funding, to D. Muñoz-Rojas and F. Gillot for assistance with CV experiments, and to M. Armand for suggestion of electrolytes and helpful discussions. We are also grateful to Electricité De France for support and discussions.

References

1. Poizot P, Laruelle S, Grugeon S, Dupont L, Tarascon JM (2000) Nature 407:496
2. Poizot P, Laruelle S, Grugeon S, Tarascon JM (2002) J Electrochem Soc 149(9):A1212
3. Badway F, Pereira N, Cosandey F, Amatucci GG (2002) J Electrochem Soc 150(9):A1203
4. Li H, Balaya P, Maier J (2004) J Electrochem Soc 151(11):A1878
5. Pfeiffer H, Tancret F, Bichat MP, Monconduit L, Favier F, Brousse T (2004) Electrochem Commun 6:263
6. Gillot F, Boyanov S, Dupont L, Doublet ML, Morcrette M, Monconduit L, Tarascon JM (2005) Chem Mater 17(25):6327
7. Pereira N, Klein LC, Amatucci GG (2002) J Electrochem Soc 149(3):A262
8. Pereira N, Balasubramanian M, Dupont L, McBreen J, Klein LC, Amatucci GG (2003) J Electrochem Soc 150(8):A1118
9. Sauvage F, Tarascon JM, Baudrin E (2007) J Phys Chem C 111:9624
10. Xu K (2004) Chem Rev 104:4303
11. Laruelle S, Pilard S, Guenot P, Grugeon S, Tarascon JM (2004) J Electrochem Soc 151(8):A1202
12. Smart MC, Ratnakumar BV, Whitacre JF, Whitcanack LD, Chin KB, Rodriguez MD, Zhao D, Greenbaum SG, Surampudi S (2005) J Electrochem Soc 152(6):A1096
13. Grugeon S, Laruelle S, Dupont L, Chevalier F, Taberna PL, Simon P, Gireaud L, Lascaud S, Vidal E, Yrieix B, Tarascon JM (2005) Chem Mater 17:5041
14. Dupont L, Grugeon S, Laruelle S, Tarascon JM (2007) J Power Sources 164:839
15. Dupont L, Laffont L, Grugeon S, Laruelle S, Bodenez V, Tarascon J-M (2007) ECS Trans 3(27):139–153
16. Muñoz-Rojas D, Leriche JB, Delacourt C, Poizot P, Palacín MR, Tarascon JM (2007) Electrochem Comm 9:708
17. Guyomard D, Tarascon JM (1992) J Electrochem Soc 139(4):937
18. Aurbach D, Zaban A, Schechter A, Ein-Eli Y, Zinigrad E, Markovsky B (1995) J Electrochem Soc 142(9):2873
19. Naoi K, Mori M, Naruoka Y, Lamanna WM, Atanasoski R (1999) J Electrochem Soc 146(2):462
20. Armand M, Gorecki W, Andreani R (1989) In: Scrosati B (ed) Proceedings of the 2nd international meeting on polymer electrolytes, vol 91. Elsevier, London
21. Favier I, Duñach E (2003) Tetrahedron Lett 44:2031
22. Laruelle S, Grugeon S, Poizot P, Dollé M, Dupont L, Tarascon JM (2002) J Electrochem Soc 149(5):A627
23. Gachot G, Grugeon S, Armand S, Pilard S, Guenot P, Tarascon JM, Laruelle S (2008) J Power Sources 178:409
24. Zhukovskii YF, Balaya P, Dolle M, Kotomin EA, Maier J (2007) Phys Rev B 76:235414
25. Bekaert E, Balaya P, Murugavel S, Maier J, Ménétrier M (2009) Chem Mater 21(5):856
26. Bonhomme F, Biensan P, Germond D, Laluque J, Laluque JM (2006) EP1619741-A1